UPGRADE OF AN INDUSTRIAL Al-BSF SOLAR CELL LINE INTO PERC USING SPATIAL ALD Al_2O_3

Floor Souren, Xavier Gay, Bas Dielissen and Roger Görtzen
SoLayTec, Dillenburgstraat 9G, 5652 AM, Eindhoven, The Netherlands
e-mail address: Floor.Souren@solaytec.com
Telephone number: +31 40 2380508

ABSTRACT: In this paper, we report the results of an upgrade from an Al-BSF solar cell line to a PERC (passivated emitter and rear cell) solar cell line, based on p-type mono-crystalline silicon (mono c-Si) material. For the rear side Al_2O_3 passivation, an InPassion ALD system of SoLayTec was used. The PERC solar cell optimization has been done in three main steps: first we optimized the rear side SiN_x capping layer, leading to a solar cell efficiency increase of $+0.4\%_{abs}$ with respect to the mono c-Si Al-BSF solar cell baseline. Secondly, we optimized the rear side polishing depth from 1-2 µm to 3-4 µm, which results in a solar cell efficiency gain of $+0.5\%_{abs}$ with respect to the standard Al-BSF solar cell baseline. For the third optimization, the emitter sheet resistance has been increased from (78±3) Ω/sq to (90±5) Ω/sq, resulting in a solar cell efficiency of (20.44±0.17)% and a gain of $>+0.8\%_{abs}$ with respect to the Al-BSF baseline. After several repeat runs, where the number of PERC solar cells has been increased to >1000 wafers per run with $>1.0\%_{abs}$ solar cell efficiency gain, >50000 PERC solar cells have been processed over two days with a stable solar cell efficiency of (20.5±0.3)% and best cell with efficiency of 21.1%. The reliability of the InPassion ALD system has been improved by decreasing the breakage rate from $0.19\%_{abs}$ to $0.05\%_{abs}$. Finally, it has been proven that with the latest configuration of the system, the breakage rate can be reduced even more to $\leq 0.05\%_{abs}$.

Keywords: PERC, ALD Al_2O_3, Manufacturing and Processing

1 INTRODUCTION

Leading PV manufacturers have started mass production of the passivated emitter and rear cell (PERC) concept within the last five years [1-3]. According to the ITRPV roadmap, the PERC solar cell concept has the largest market share of ~10% of all advanced solar cell concepts [4]. In addition, the ITRPV roadmap predicts that the PERC solar cell concept will also have the largest increase in market share: to up to 20% in 2017 and to up to >30% in 2019 [4]. One of the main reasons for this is that the PERC solar cell design leads to a solar cell efficiency increase of $0.5\%_{abs}$-$0.8\%_{abs}$ based on p-type multi-crystalline Si (mc-Si) material and $0.6\%_{abs}$-$1.0\%_{abs}$ based on p-type mono crystalline Si (mono c-Si) material with respect to the standard Al-BSF solar cell, respectively. An additional benefit of the PERC solar cell concept is that it can be relatively easily implemented on a conventional screen printing Al-BSF Si solar cell manufacturing line. Additional tools for PERC are a rear side passivation system to deposit the Al_2O_3, a post-deposition annealing tool, a tool for rear side SiN_x capping and a laser. For the rear side SiN_x capping layer, the tool for SiN_x anti reflection coating, which is available in the standard Al-BSF solar cell line, can be used. The post-deposition annealing step can be integrated in the SiN_x capping process. It is optional to upgrade the edge isolation tool to increase the polishing depth from 1-2 µm to 3-4 µm [5,6,7].

In this paper we report on an upgrade of an Al-BSF solar cell line into PERC, based on mono c-Si material. Several runs have been performed to optimize the PERC solar cell process and after several repeat runs, for the final PERC run >50000 PERC solar cells have been produced.

2 EXPERIMENTAL SETUP

2.1 Solar cell processing flow

For the upgrade of the standard Al-BSF solar cell into a mono c-Si PERC solar cell line, based on p-type Czochralski Si wafers (156 mm·156 mm, 1-3 Ω·cm), the following equipment is added: an InPassion ALD of SoLayTec for rear side ALD Al_2O_3 passivation, a laser for rear side contact opening, and an upgrade of the edge isolation to increase the polishing depth from 1-2 µm to 3-4 µm. The system for the SiN_x anti-reflection coating was also used for the deposition of rear side SiN_x capping layer on the ALD Al_2O_3 layer. The deposition time of the SiN_x anti reflection coating, which is at a thickness between 70 nm and 80 nm, has been increased to deposit a thickness of the SiN_x capping layer with a value between 100 nm and 150 nm. The post-deposition annealing has been done external, but can be integrated in the rear side SiN_x capping process. Originally, the standard Al-BSF solar cell line was based on mc-Si material and, therefore, for the upgrade into mono c-Si PERC solar cells, the saw damage removal and texturing step has been changed from acidic etching to alkaline etching. In order, to have a proper comparison between PERC and Al-BSF, the mc-Si Al-BSF baseline was converted to mono c-Si Al-BSF and all results presented in this paper are based on mono c-Si material. An overview of the processing sequences for the mono c-Si PERC solar cells versus the mono c-Si Al-BSF solar cells is presented in Figure 1.

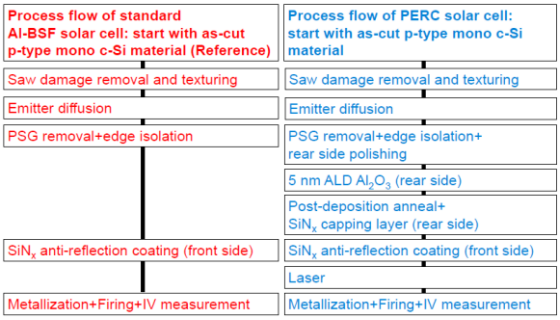

Figure 1: Processing flows for the Al-BSF solar cell and PERC solar cell.

2.2 ALD Al_2O_3 equipment

The ALD equipment of SoLayTec is based on six identical modules with a gross throughput of 3600 wafers/hour at an ALD Al_2O_3 layer thickness of 4.7 nm. An image of the six modules ALD system is presented in Figure 2.

Figure 2: InPassion ALD equipment of SoLayTec, which consists of six modules, with loader and unloader.

The wafers are placed on the main conveyor belt via a loader system. The main belt transports the wafers to one of the six deposition modules. In a module, the wafer is first in a pre-heating stage where it is heated to the desired processing temperature of 200°C and successively the wafer starts floating on air. In the next step, the wafer is transported into the reactor to deposit Al_2O_3 layer via spatial ALD [8]. Floating on air, the wafer is moving back and forward, and for each pass, the wafer is going through the different reactor zones. The reactor zones consist of a consecutive exposure to: H_2O, TMA (=trimethylalumium), H_2O, TMA and, again H_2O, separated by N_2 to prevent the mixing of precursors. Schematic overview of the injector head is presented in Figure 3.

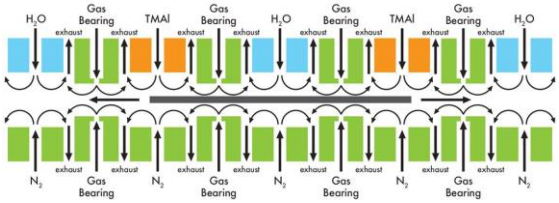

Figure 3: Schematic cross section of the injector head of the spatial ALD reactor.

Per pass through the injector head, 2 layers of ALD Al_2O_3 are deposited leading to a typical deposition rate of 1 nm/s. The deposition thickness can be controlled by setting the number of passes. After deposition of the requested layer thickness, the wafer is cooled down and placed back on the main conveyor belt and finally to the unloader system. The modules can process independently from each other to ensure the maximum up-time.

3 RESULTS

3.1 PERC optimization runs

The first PERC processing run resulted in a solar cell efficiency of 0.4%$_{abs}$ lower than the Al-BSF solar cell. We have optimized the solar cell efficiency of the PERC cell in three main optimization steps, SiN_x capping optimization, polish depth optimization, and emitter sheet resistance optimization. First, we optimized the SiN_x capping layer deposited on the ALD Al_2O_3, which has led to a solar cell efficiency increase of 0.4%$_{abs}$ with respect to the standard Al-BSF solar cell. The results are presented in Table I. The PERC solar cell efficiency increase is caused by an improvement in rear side passivation quality and optimized rear side reflection, resulting in an 3 mV increase of the open circuit voltage and an 1.2 mA/cm^2 increase of the short circuit current density, respectively.

Table I: Overview of solar cell efficiency parameters for the standard Al-BSF solar cell and for the PERC solar cell with rear side SiN_x capping recipe A and B, respectively. The open circuit voltage (V_{oc}), short circuit current density (j_{sc}), series resistance (R_s), shunt resistance (R_{sh}), fill factor (FF) and solar cell efficiency (η) show a clear improvement with optimized SiN_x capping recipe.

	Standard Al-BSF	PERC SiN_x capping recipe A	PERC SiN_x capping recipe B
V_{oc} (mV)	631±1	632±2	634±2
j_{sc} (mA/cm^2)	38.1±0.2	39.2±0.2	39.3±0.2
R_s (mΩ)	3.0±0.3	3.9±0.2	4.0±0.3
R_{sh} (Ω)	164±47	47±11	75±34
FF (%)	79.2±0.4	77.7±0.5	78.0±0.6
η (%)	19.06±0.17	19.27±0.20	19.44±0.23
Number of solar cells	42	27	31

In the second optimization step, we increased the rear side polishing depth from 1-2 µm to 3-4 µm and thereby increased the solar cell efficiency gain to 0.5%$_{abs}$ with respect to the standard Al-BSF solar cell. The additional efficiency gain was related to an improved open circuit voltage as well as to an improved fill factor difference between PERC and the Al-BSF solar cell. A smaller surface area leads to less dangling bonds which results in less surface recombination and, therefore, to a lower surface recombination velocity and to an increase of the open circuit voltage. The increase of polishing depth from 1-2 µm to 3-4 µm leads to a smaller silicon surface area and, therefore, to an increase of the open circuit voltage. The results are presented in Table II.

Table II: Overview of solar cell efficiency parameters for the standard Al-BSF and PERC solar cell with increased etch depth of 3-4 µm.

	Standard Al-BSF	PERC 3-4 µm polishing
V_{oc} (mV)	632±1	636±2
j_{sc} (mA/cm^2)	39.0±0.1	40.2±0.1
R_s (mΩ)	3.4±0.3	4.1±0.4
R_{sh} (Ω)	103±48	148±42
FF (%)	78.3±0.4	77.7±0.5
η (%)	19.32±0.11	19.85±0.16
Number of solar cells	39	39

In the third optimization step, we increased the sheet resistance of the emitter from (78±3) Ω/sq to (90±5) Ω/sq by decreasing the diffusion temperature of the diffusion process. The results are presented in Table III. The PERC solar cell with optimized emitter sheet resistance of (90±5) Ω/sq showed a higher solar cell efficiency of

0.2%$_{abs}$ with respect to the PERC solar cell with standard emitter sheet resistance of (78±3) Ω/sq. This increase is caused by a higher open circuit voltage of 3 mV while maintaining the fill factor. Based on this result, we concluded that the limiting factor of the PERC solar cell was recombination losses in the emitter. By increasing the sheet resistance of the emitter, the losses of minority carriers in the emitter were reduced, which led to an increase of the open circuit voltage. Because of a similar fill factor of the PERC group with increased sheet resistance of (90±5) Ω/sq compared to the PERC group with standard sheet resistance (78±3) Ω/sq, we can conclude that the PERC group with higher sheet resistance can be contacted properly. The emitter optimization led to a total increase in solar cell efficiency for PERC of 0.8%$_{abs}$ compared to the standard Al-BSF solar cell. The obtained gain in open circuit voltage and short circuit current density are 12 mV, and 1.5 mA/cm^2 respectively. Note that for the optimized emitter sheet resistance, a loss in fill factor of 1.1%$_{abs}$ with respect to the standard Al-BSF solar cell was obtained.

Table III: Overview of solar cell efficiency parameters for the standard Al-BSF solar cell and for the PERC solar cell with standard and optimized emitter sheet resistance of (78±3) Ω/sq and (90±5) Ω/sq, respectively.

	Standard Al-BSF	PERC with standard emitter sheet resistance $R_{standard\_sheet}$ =(78±3)Ω/sq	PERC with optimized emitter sheet resistance $R_{optimized\_sheet}$ =(90±5)Ω/sq
V_{oc} (mV)	635±2	644±3	647±3
j_{sc} (mA/cm^2)	38.5±0.1	39.9±0.1	40.0±0.1
R_s (mΩ)	2.1±0.1	2.6±0.2	2.8±0.2
R_{sh} (Ω)	162±74	94±29	96±30
FF (%)	80.1±0.1	79.0±0.3	79.0±0.3
η (%)	19.61±0.10	20.28±0.18	20.44±0.17
Number of solar cells	40	37	39

In Figure 4a, the solar cell efficiency of the PERC and Al-BSF baseline is presented for the different optimization steps as discussed before, followed by three repeat runs. In Figure 4b, the same data are presented, but the solar cell efficiency of PERC and the Al-BSF solar cell is presented relative to each other. For the optimization runs as well as for the first repeat run, the number of wafers per group were relatively small at <100 wafers. For the second and third repeat run, the number of PERC solar cells was increased to 1100 and 1340 wafers, respectively. The open circuit voltage (V_{oc}), short circuit current (j_{sc}) and fill factor (FF) of the optimization and repeat runs are presented in Figure 5a, 5b and 5c, respectively. The increase of the solar cell efficiency for PERC and the Al-BSF solar cell for the repeat runs 2 and 3 compared to repeat run1 are caused by an increase of the open circuit voltage as well as by an increase of the fill factor. Different and better wafer material leads to an increase of the open circuit voltage and an optimized firing condition results in an improved fill factor.

a)

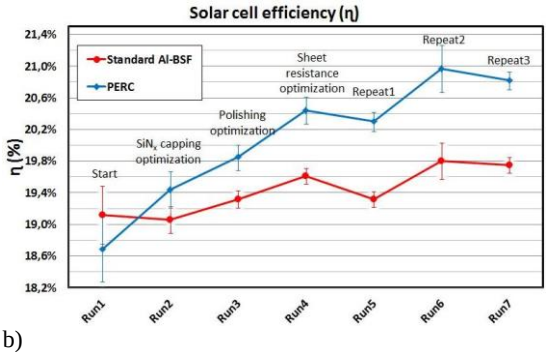

b)

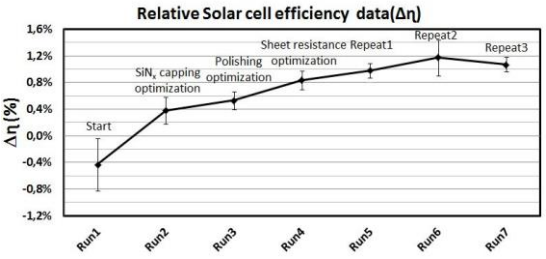

Figure 4: Absolute solar cell efficiency (a) and the solar cell efficiency of PERC and Al-BSF solar cell relative to each other (b).

a)

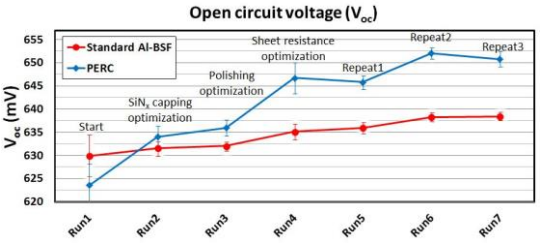

b)

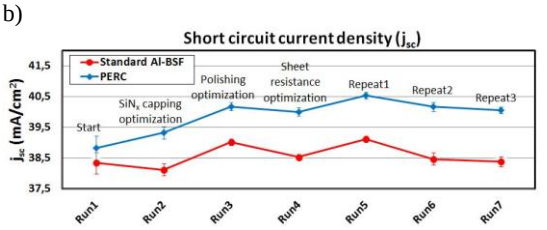

c)

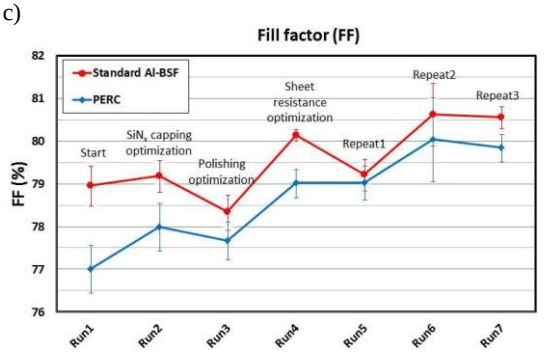

Figure 5: Open circuit voltage (V_{oc}) (a), short circuit current density (j_{sc}) (b), and fill factor (FF) (c) for PERC solar cell and standard Al-BSF solar cell for the different optimization runs and repeat runs.

3.2 PERC production ramp-up

Finally, production ramp-up was initiated and over 2 days >50000 PERC solar cells have been manufactured. Figure 6 shows the efficiency of the solar cells with

average solar cell efficiency of (20.5±0.3)% and the best PERC cell reaches 21.1%. The cell distributions of day 1 and day 2 are fitted to a normal distribution, as presented in Figure 7a and Figure 7b, respectively. The solar cell efficiency distribution is as expected for solar cells: a faster drop off for the higher efficiency cells and a slower drop off for the lower efficiencies, which means that there are relatively more bad cells than would be expected from a perfect normal distribution. From the fitted normal distribution, the average solar cell efficiency (μ_{normal}), the standard deviation (σ_{normal}) as well as the full width at half maximum ($FWHM_{normal}$) are determined. For day 1 and day 2, the average efficiency is equal to (20.6±0.2)%, which is slightly higher than the average value of the solar cell efficiency data and can be explained by the fact that for the normal distribution there are less low fliers compared to the solar cell efficiency data. For day 1 and day 2, the standard deviation and full width at half maximum are determined to be at 0.2%$_{abs}$, and 0.4%$_{abs}$, respectively. The FWHM of the normal distribution is similar to the FWHM of mono c-Si PERC solar cells as published by Trina, showing the relatively good quality of the solar cell line [9]. In this paper, we show the results of the successful upgrade into mono c-Si PERC solar cells originally starting from a mc-Si Al-BSF solar cell line instead of a mono c-Si Al-BSF line. Where the results presented in this paper for PERC and Al-BSF solar cells are all based on mono c-Si material to make a correct comparison.

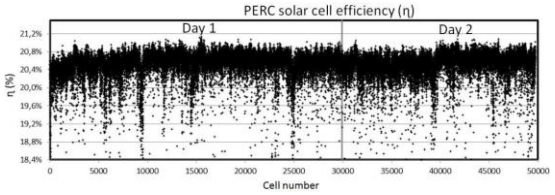

Figure 6: Absolute solar cell efficiency of the first 2 days of the production ramp-up of PERC. A stable efficiency of (20.5±0.3)% has been achieved.

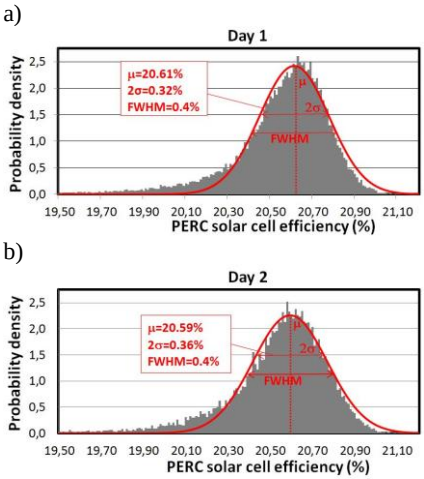

Figure 7: Probability density of PERC solar cell efficiency for day 1 (a) and day 2 (b), where for both days based on the normal distribution the average solar cell efficiency is at 20.6% and FWHM is determined to be on 0.4%. FWHM is the width of the distribution where the distribution is equal to half of the maximum.

The corresponding open circuit voltage (V_{oc}), short circuit current (j_{sc}), and fill factor (FF) of the PERC solar cells, are presented in Figure 8a, 8b and 8c, respectively.

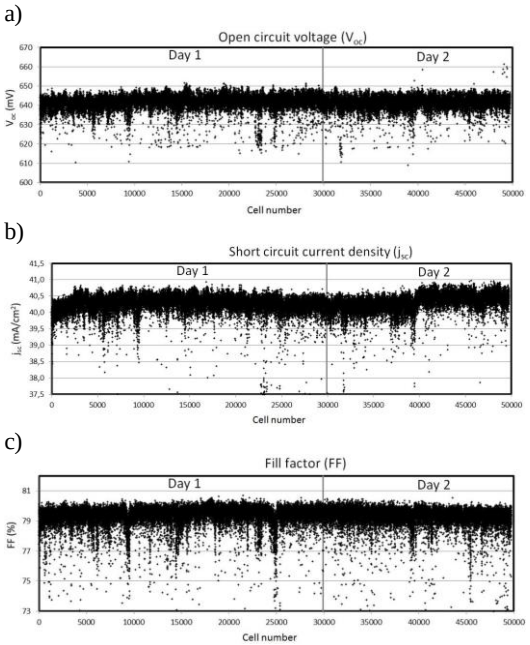

Figure 8: Open circuit voltage (V_{oc}) (a), short circuit current density (j_{sc}) (b), and fill factor (FF) (c) of the first 2 days of the production ramp-up of PERC.

Of all the results of open circuit voltage, short circuit current density and fill factor, the fill factor has the widest distribution, with a lot of low fliers (e.g. around cell numbers: 10000, 15000, 25000, 40000 and 45000) leading also to low fliers in the solar cell efficiency. This indicates that for further increase of the solar cell efficiency, the fill factor needs to be improved, which shows also the further optimization potential. Moreover, the PERC solar cell efficiency increases with ca 0.1%$_{abs}$ for the first couple of 1000 solar cells of day 1 and at day 2 after ~40.000 cells, which corresponds to an increase of the short circuit current density. Open circuit voltage has the smallest distribution, which shows that the passivation with ALD Al_2O_3–SiN_x stack is performing well. Overview of the solar cell efficiency parameters and parameters which characterize the normal distribution are presented in Table IV.

Table IV: Overview of solar cell efficiency parameters for the PERC production of day 1 and day 2, respectively. The solar cell efficiency distribution has been fitted according normal distribution and from this distribution, the average solar cell efficiency ($\eta_{average\_normal}$), standard deviation (σ_{normal}) and full width at half maximum ($FWHM_{normal}$) have been determined.

	PERC production day 1	PERC production day 2
V_{oc} (mV)	642±4	641±3
j_{sc} (mA/cm^2)	40.3±0.3	40.3±0.3
FF (%)	79±1	79±1
η_c (%)	20.5±0.4	20.5±0.3
Number of solar cells	29918	19830
	Fit with Normal distribution:	Fit with Normal distribution:
η_{normal} (%)	20.6	20.6
σ_{normal} (%)	0.2	0.2
$FWHM_{normal}$ (%)	0.4	0.4

3.3 Reliability improvement of InPassion ALD

Over the last few months, the reliability of the InPassion ALD of SoLayTec has been significantly improved, which is presented by the breakage rate in Figure 9. The breakage rate is monitored on a production level of more than 75000 wafers per day. The Module-type 2015 reached an average wafer breakage rate of 0.19%$_{abs}$, while the module-type 2015+ shows a reduced breakage rate at an average value of 0.05%$_{abs}$. Preliminary results present that for the Module-type 2016, the average breakage rate has been decreased even more to ≤0.05%$_{abs}$ which is based on 5000 wafers per day for a few consecutive days.

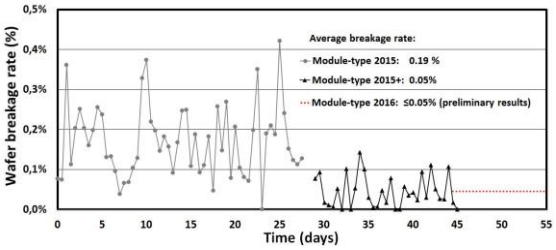

Figure 9: Wafer breakage rate as function of days for 3 different module types: Module-type 2015, Module-type 2015+ and Module-type 2016.

4 CONCLUSIONS

Ramp-up of PERC solar cell line based on p-type mono c-Si material has been done in three optimization steps: optimization of rear side SiN_x capping process, the rear side polishing depth, and optimization of the emitter sheet resistance. After the third optimization, the solar cell efficiency for PERC was determined at (20.44±0.17)%, which was >0.8%$_{abs}$ higher with respect to the standard Al-BSF solar cell reference. Successfully, for two repeat runs, even >1.0%$_{abs}$ solar cell efficiency gain has been obtained caused by an increase of wafer quality and optimized firing condition. Finally, >50000 PERC solar cells have been processed at average solar cell efficiency of (20.5±0.3)% where the solar cell efficiency distribution has been fitted to a normal distribution, showing an average value of (20.6±0.2)% and $FWHM_{normal}$ of 0.4%$_{abs}$, and this value is similar as presented by Trina for mono c-Si PERC, and shows that the ramp-up was successful. These results show also that implementation of mono c-Si PERC solar cell can be done successful starting from a mc-Si Al-BSF solar cell line. All results of Al-BSF solar cells and PERC solar cells presented in this paper, are based on mono c-Si material. Based on these >50000 PERC solar cells, the parameter with widest distribution and most low fliers is the fill factor and shows further optimization potential which can increase solar cell efficiency. The parameter with the smallest distribution is the open circuit voltage, which is caused by the good rear side passivation of the ALD Al_2O_3-SiN_x stack. Together with an improved breakage rate down to ≤0.05%$_{abs}$ of the InPassion ALD, SoLayTec offers an interesting solution for mass production of ALD Al_2O_3 for PERC solar cells.

5 REFERENCES

[1] D. Chen et al., 21.40% Efficient Large Area Screen Printed Industrial PERC Solar Cells, 30th European Photovoltaic Solar Energy Conference and Exhibition, Hamburg, Germany.

[2] J.W. Müller et al., Current Status of Q-Cells' High-Efficiency Q.ANTUM Technology with New World Record Module Results, 27th European Photovoltaic Solar Energy Conference and Exhibition, Frankfurt, Germany.

[3] B. Tjahjono et al., Optimizing Celco Cell Technology in one Year of Mass Production, 28th European Photovoltaic Solar Energy Conference and Exhibition, Paris, France.

[4] International Technology Roadmap for Photovoltaic (ITRPV) 2015, 6th edition, April 2015.

[5] R. Sastrawan et al., Implementation of a Multicrystalline ALD-Al_2O_3 PERC-Technology into an Industrial Pilot Production, 28th European Photovoltaic Solar Energy Conference and Exhibition, Paris, France.

[6] D. Pysch et al., Implementation of an ALD-Al_2O_3 PERC-Technology into a Multi- and Monocrystalline Industrial Pilot Production, 29th European Photovoltaic Solar Energy Conference and Exhibition, Amsterdam, The Netherlands.

[7] Xavier Gay et al., Post-Deposition Thermal Treatment of Ultrafast Spatial ALD Al_2O_3 for the Rear Side Passivation of p-type PERC Solar Cells, 28th European Photovoltaic Solar Energy Conference and Exhibition, Paris, France.

[8] Poodt et al. High-Speed Spatial Atomic-Layer Deposition of Aluminum Oxide Layers for Solar Cell Passivation, Advanced Materials, 22(32), 3564-3567, 2010.

[9] D. Chen et al., 21.40% Efficient Large Area Screen Printed Industrial PERC Solar Cell, 31st European Photovoltaic Solar Energy Conference and Exhibition, Hamburg, Germany.